Preparation and Characterization of a Composite Paste Composed of Ag-Coated Cu Nanoparticles and Non-Particle-Based Ag Ink

Woo Lim Choi and Jong-Hyun Lee*

*Department of Materials Science and Engineering, Seoul National University of Science and Technology,
Seoul 01811, Republic of Korea*

With the aim of forming thick films with excellent electrical conductivity using a binder-free paste formulation, a novel composite paste composed of ∼195 nm Ag-coated Cu nanoparticles and non-particle-based Ag ink was developed. The Ag-coated Cu nanoparticle/21 wt% Ag composite paste exhibited improved properties that could not be accomplished using the non-particle-based Ag ink alone; the film thickness and sheet resistance were 129.2 nm and 0.184 $\Omega/\square$, respectively, even after brief sintering for 10 min at 150 °C. The Ag precipitated from the Ag ink in the composite pastes formed not only bumpy shells on the surfaces of the Ag-coated Cu nanoparticles but also connections between the particles during sintering. Although the sintered composite film presented a porous microstructure by solvent evaporation from the ink, a surface hardness of 470 MPa was obtained.

Keywords: Composite Paste, Ag-Coated Cu Nanoparticle, Ag Ink, Film Thickness, Sheet Resistance.

1. INTRODUCTION

With the prevalence of the printed electronics industry, the use of Ag ink and paste is consistently increasing to form various conductive patterns or electrodes on surfaces directly.[1–3] Although ink type is important in terms of achieving fine patterning, the ink cannot form a thick film.[4] However, the paste can be transformed into a thick film by a single printing process depending on the mask thickness and filler size. In ordinary pastes, the thickness of the film patterned by printing is retained with the help of sticky ingredients such as binders. However, the organic binder tends to settle in interfaces or voids between conductive fillers, even after curing, eventually reducing the electrical conductivity of the consolidated film considerably.[5]

To enhance the electrical conductivity in consolidated films fabricated by using paste, removal of the organic binder in the paste formulation or elimination of organic ingredients during consolidation of the film is required.[6–8] However, removal of the organic binder is detrimental to the rheological properties of the paste and requires long sintering times at higher temperatures.[9] The elimination of organic ingredients also demands a long sintering process at even higher temperatures.[10]

Ag particles of various shapes and sizes have been used as the main filler material in conductive pastes.[12–15] However, the high material cost of Ag has also been a crucial obstacle suppressing the use of these materials. Although Cu is a promising material in terms of electrical and thermal conductivity, the oxidation nature of Cu still restricts its application as a filler material.[16, 17] Consequently, film fabrication with short sintering times at low temperatures of approximately 150 °C using binder-free formulations and a low-cost filler material that results in thick films with excellent electrical conductivity is urgently required.

In this study, a novel composite paste made by mixing Ag-coated Cu particles several hundred nanometers in size and a commercial Ag ink that did not contain Ag nanoparticles was prepared and the processibility and electrical/mechanical properties of the resultant films were evaluated. The Ag ink contained soluble Ag cluster complexes instead of Ag nanoparticles, and thus Ag nanoparticles precipitated from the ink during heat treatment at approximately 150 °C.[18] The precipitation behavior was anticipated to enhance the sinterability of the novel composite paste. It was also expected that the Ag shells of the Ag-coated Cu nanoparticles would prevent oxidation of the core Cu particles during sintering. With a distinctive precipitation/sintering mechanism of the Ag ink,

---

*Author to whom correspondence should be addressed.

the microstructural properties of the sintered composite films and the sintering mechanism of the composite paste are discussed. In addition, the electrical conductivities and surface hardness values of the sintered films with different mixing ratios are presented.

2. EXPERIMENTAL DETAILS

Cu nanoparticles approximately 200 nm in size were synthesized in-house using a retained wet reduction method. Then, the Cu nanoparticles were coated with Ag shells by electroless plating to prepare Ag-coated Cu nanoparticles approximately 200 nm in size, which were used as the main filler material. For the plating, 9.53 g of Cu particles were dispersed in 300 mL of polyol solution by stirring. The Ag coating process was performed by the three-step addition of a Ag precursor solution and a reductant. 2 mM of L-ascorbic acid ($C_6H_3O_6$, reagent grade, Aldrich Chemical Co.) as the reductant was first dissolved in the Cu particle solution. The Ag precursor solution was prepared by completely dissolving 5.9 mM of silver nitrate ($AgNO_3$, 99.8%, Sooshin Chemical Co., Ltd.) in 10 mL of ammonium hydroxide (NH_4OH, 28–30%, Samchun Pure Chemical Co., Ltd.). The Ag precursor solution was added drop-wise into the Cu solution at an injection rate of 3.3 mL/min under continuous stirring at 300 rpm at room temperature. After maintaining the reaction for 10 min, another 10 mL of the Ag precursor solution was added; this addition was repeated three times in total to form 15 wt% Ag shells. The mixed final solution was continuously stirred for 30 min and then centrifuged at 7000 rpm for 2 min. Ethanol (C_2H_5OH, 95%, Korea Alcohol Industrial Co., Ltd.) was then used to wash the formed Ag-coated Cu nanoparticles after the supernatant was decanted. The Ag-coated Cu nanoparticle slurry obtained after washing with ethanol three times was dried at room temperature in a vacuum chamber. The shape and surface morphology of the prepared Cu and Ag-coated Cu nanoparticles were examined using a field-emission scanning electron microscope (FE-SEM, SU8010, Hitachi High Technologies Corporation). Phase and crystal structure of the prepared particles were also confirmed using X-ray diffractometer (XRD, JP/MAX-3C, Rigaku Denki Co., Ltd.).

TEC-IJ-060 Ag ink (InkTec Co., Ltd.) was selected as the vehicle to be added to the paste formulation. The Ag ink did not contain Ag nanoparticles but rather soluble Ag cluster complexes.[19] The fabricated Cu and Ag-coated Cu nanoparticles were mixed with the Ag ink for 30 min using a spatula. Samples were fabricated where the amount of Ag ink added to the Ag-coated Cu nanoparticles was 15, 17, 19, and 21 wt%. The prepared composite pastes were printed on Si wafers using a stencil mask (thickness: 100 μm) containing a 10×10 mm hole. The printed patterns were annealed at 150 °C for 10 min in air atmosphere using a box furnace. The Ag ink was also coated on a

Si wafer using a spin coater (Spin-1200D, Midas System Co., Ltd.) to prepare a pure Ag film in order to compare the properties of the sintered films. The spin coating consisted of three steps: the first and second steps were conducted for 5 s at 500 and 1000 rpm, respectively. The third step was performed for 30 s at 2000 rpm. The cross sections and surface microstructures of the sintered films were checked using a FE-SEM (JSM-6700F, JEOL Ltd.). The electrical conductivities of the surfaces of the sintered films were measured by a four-point probe method with a source meter (2400, Keithley Instruments Inc.). Lastly, the mechanical robustness of the surfaces of the sintered films was evaluated using a nanoindenter (Nanotest NTX, Micro Materials).

3. RESULTS AND DISCUSSION

Figures 1(a) and (b) show SEM images of the synthesized Cu and Ag-coated Cu nanoparticles, respectively (the phase and crystal structure of each particle sample were confirmed by Fig. 1(c)). Both particles exhibited a polygonal shape; however, the Ag-coated Cu particles showed very rough surfaces owing to the Ag plating. Both particle sizes were approximately 200 nm (Cu: 189.4 ± 31.0 nm, Ag-coated Cu: 194.6 ± 42.0 nm) because the thickness of the Ag shell was estimated to be less than 10 nm.[20] For both types of nanoparticles, it was found that the aggregation between the particles was extremely suppressed. Moreover, the results in Figure 1(c) indicated the formation of pure Cu and Ag-coated Cu nanoparticles without significant oxides.
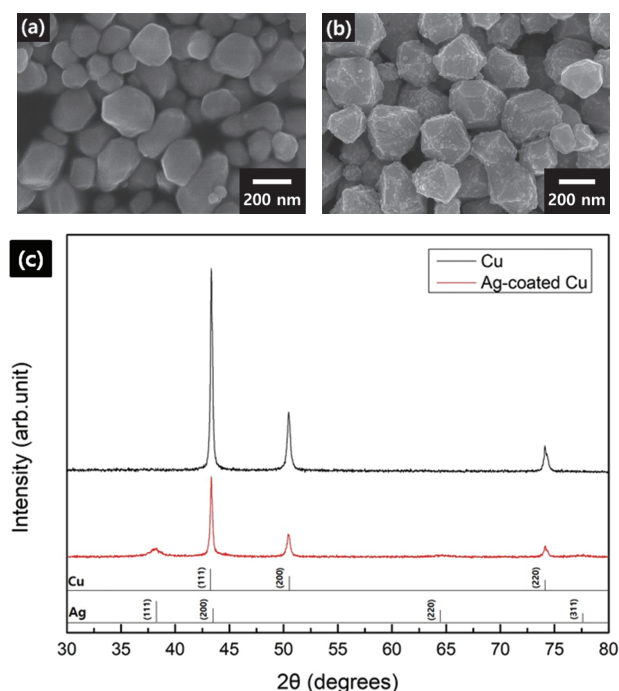

Fig. 1. SEM images of (a) Cu and (b) Ag-coated Cu nanoparticles synthesized in-house, (c) XRD patterns of the particles.
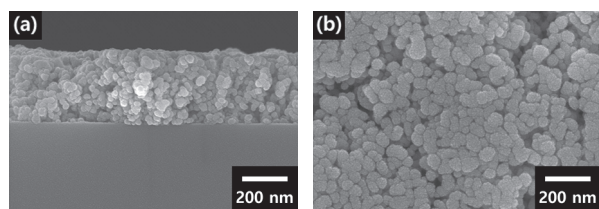
Fig. 2. SEM images of (a) cross section and (b) surface of a sintered pure Ag film.

Figures 2(a) and (b) show the cross-section and surface images of the pure Ag film sintered after spin coating of the Ag ink. During annealing at 150 °C, pure Ag nuclei were formed initially and then the nuclei grew to fine particles through the additional supply of Ag atoms during the ink formulation. Then, the agglomeration behavior between the grown particles induced formation of bigger particles, which were sintered together during the final stage. Consequently, the average grain size in the sintered film was measured to be 55 ± 10 nm. Furthermore, the thickness of the film was 317.1 ± 6.6 nm and the sheet resistance was found to be 0.487 ± 0.03 $\Omega/\square$.

A representative image of the cross section of the film sintered after stencil printing of the Ag-coated Cu nanoparticle/21 wt% Ag composite paste is shown in Figure 3. The conductive film was formed through a process in which the precipitation of fine Ag particles from the added Ag ink coincided with sintering between the Ag-coated Cu nanoparticles. Thickness of the film was 129.2 ± 3.7 μm, which is approximately 407 times thicker than that of the pure Ag film. The formation of a thick conductive film consisting of only the metallic constituent by stencil printing just one time can be considered a representative property of this composite paste. The film thickness increased with increasing Ag ink amount, and the final thickness of the sintered film surpassed the initial thickness of the printed film when the Ag ink amount was 21 wt%. This distinctive result might have occurred as a result of the slight floating phenomenon of the Ag-coated Cu nanoparticles by solvent evaporation from the Ag ink during sintering. The Ag ink converted to Ag nanoparticles immediately after vaporization of the solvent during sintering. If vaporization of the solvent caused slight flotation
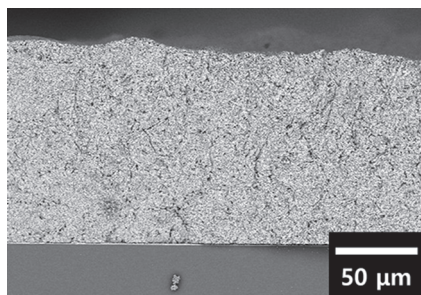

Fig. 3. Cross-sectional SEM image of the film fabricated with Ag-coated Cu nanoparticle/21 wt% Ag composite paste.
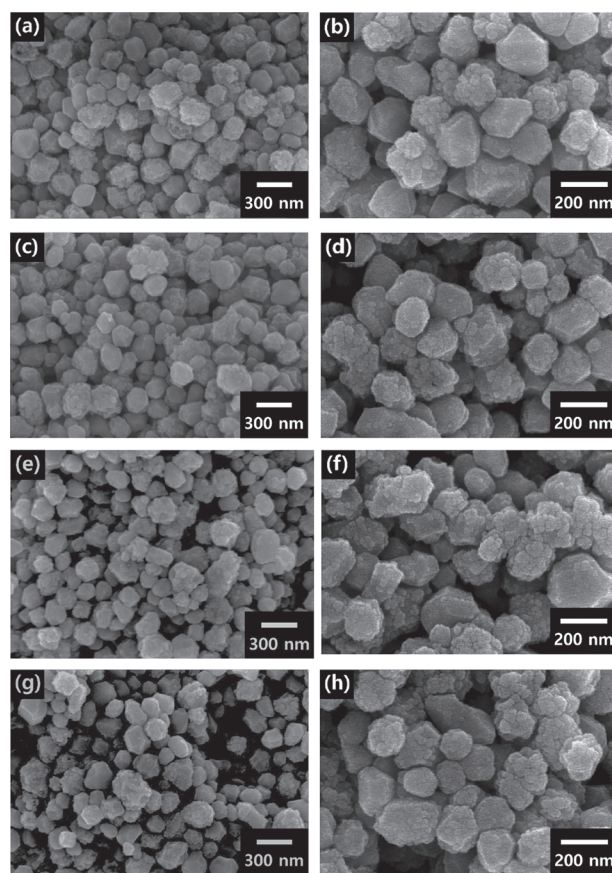

Fig. 4. (a, c, e, g) Cross-section and (b, d, f, h) surface SEM images of Ag-coated Cu particle/Ag composite films with different amounts of Ag ink: (a, b) 15, (c, d) 17, (e, f) 19, and (g, h) 21 wt%.

of Ag-coated Cu nanoparticles $\sim$195 nm in size, Ag would precipitate from the Ag ink and formation of a swelled film with the porous microstructure observed in Figures 3 and 4 would result.

Figure 4 displays magnified images of the cross sections and surfaces of the composite films with respect to the amounts of Ag ink added. Although the density of the cross-section microstructure was higher than that of the surface for the same film, the densities of the films were not high. However, the connectivity between the Ag-coated Cu nanoparticles was enhanced with increasing Ag ink amount. As per the above-mentioned sintering mechanism, the low density was primarily attributed to the slight floating phenomenon of Ag-coated Cu nanoparticles by solvent evaporation in the Ag ink during sintering. In such a situation, the volume of pure Ag precipitated from the Ag ink would be insufficient to fill the spaces between floating Ag-coated Cu nanoparticles. Actually, the Ag generated from the Ag ink in the composite paste did not form particles, as observed in Figure 2, but rather shell layers on the Ag-coated Cu nanoparticles. Heterogeneous precipitation such as the formation of a shell layer is more favorable with a lower energy barrier compared to homogeneous precipitation such as the formation of

particles.[21] Consequently, the surfaces of the Ag-coated Cu nanoparticles showed a different morphology with a covering of bumpy Ag. The coverage of the bumpy Ag increased in proportion to the increase of added Ag ink amount, and thus the connectivity between the Ag-coated Cu nanoparticles also increased with increasing Ag ink amount. Because stable printability of the composite paste was required, the addition of Ag ink exceeding ∼21 wt% was not conducted. The lower density observed on the surfaces of the sintered films seemed to be due to the small quantity of Ag ink in the exposed surface, unlike the situation in which Ag-coated Cu nanoparticles sank under Ag ink in the interior.

Figure 5 presents the sheet resistances of the composite films with different amounts of Ag ink. The resistance decreased faster as the amount of Ag ink added increased. The number of electrical paths that can be formed between Ag-coated Cu nanoparticles and the average cross-sectional area per path were increased by the enhanced connectivity between the particles, which in turn was caused by the increased amount of precipitated Ag. The microstructural change actively contributed to the increase of electrical conductivity. Specifically, the resistance of the Ag-coated Cu particle/21 wt% Ag composite film was 0.184 $\Omega/\square$, which is a remarkable improvement when compared with that of the sintered pure Ag film shown in Figure 2 (0.487 $\Omega/\square$). The enhancement is mainly attributed to the decrease in the number of interfaces per unit volume by the addition of relatively big Ag-coated Cu nanoparticles.

To confirm the effectiveness of the Ag shells coating the Ag-coated Cu particles, a film sintered with a Cu particle/21 wt% Ag composite paste was also prepared. Figure 6 presents the back-scattered electron images of the sintered composite film. Similar to the results in the Ag-coated Cu particle/Ag composite paste, Ag precipitated from Ag ink formed on the Cu particles. However,
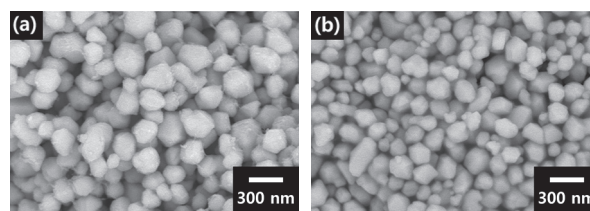

Fig. 6. Back-scattered electron images of the film sintered with Cu nanoparticle/21 wt% Ag composite paste: (a) Cross section and (b) surface.

the shape of the precipitated Ag was significantly different from that of the precipitated Ag in the Ag-coated Cu particle/Ag composite paste; tiny and irregular Ag precipitates that looked like dust and fur were observed on the Cu surfaces instead of the bumpy Ag shells. The irregularity and extremely low coverage of Ag can be explained as the result of oxidation of the Cu surfaces during sintering. It has been reported that the formation of a Cu oxide layer on the Cu surface hinders the Ag coating behavior.[22] The sheet resistance of the film was also extremely high, approximately 25 $\Omega/\square$, owing to the oxidation.

To evaluate the mechanical robustness of the composite films, the surface hardness values of the films were evaluated by the nanoindentation method. The hardness values can be interpreted as the stress required to crack the surfaces of the sintered films. The surface hardness results of the Ag-coated Cu particle/Ag composite films with respect to the amounts of Ag ink are displayed in Figure 7. The hardness increased as the amount of Ag ink increased from 15 wt% to 21 wt%. In particular, the value increased considerably to 470.0 ± 30.5 MPa for the Ag amount of 21 wt% with an increase in the amount of precipitated Ag. Simultaneously considering the result of Figure 5, the optimal Ag content in the Ag-coated Cu particle/Ag composite paste was determined to be 21 wt%.
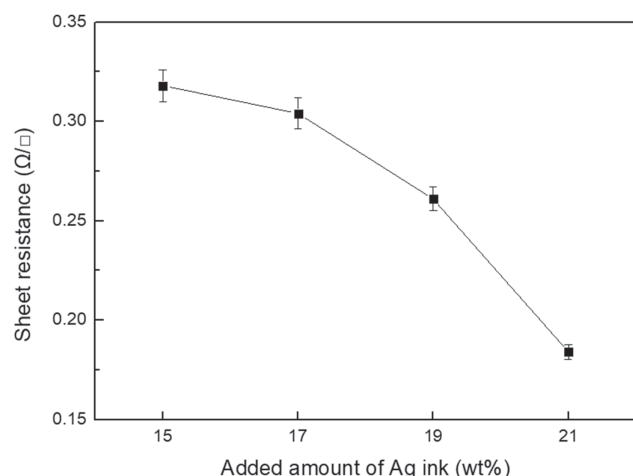

Fig. 5. Sheet resistances of Ag-coated Cu particle/Ag composite films with different amounts of Ag ink.
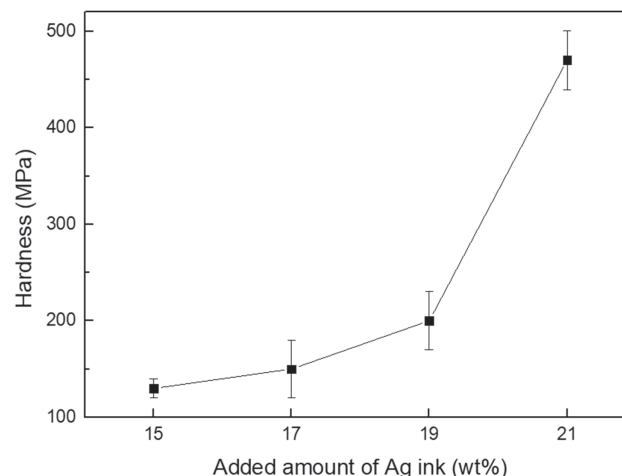

Fig. 7. Surface hardness values of Ag-coated Cu particle/Ag composite films with different amounts of Ag ink.

4. CONCLUSION

To fabricate thick films with excellent electrical conductivity using a short sintering time at low temperature, a novel composite paste with a binder-free formulation was developed. The paste was prepared by mixing ∼195 nm Ag-coated Cu nanoparticles and non-particle-based Ag ink. The Ag-coated Cu nanoparticle/21 wt% Ag composite paste showed a film thickness of 129.2 nm and a sheet resistance of 0.184 $\Omega/\square$, even after short sintering for 10 min at 150 °C. The thickness and resistance were significantly improved with increasing amounts of Ag ink. The Ag precipitated from the Ag ink in the composite pastes created bumpy shells on the surfaces of the Ag-coated Cu nanoparticles and simultaneously made connections between the particles during sintering. Even though the sintered composite film showed low density of the porous structure, a surface hardness approaching 470 MPa was measured.

References and Notes

1. L. Balan, J.-P. Malval, R. Schneider, and D. Burget, *Mater. Chem. Phys.* 104, 417 (**2007**).
2. J.-T. Tsai and S.-T. Lin, *J. Alloys Compd.* 548, 105 (**2013**).
3. S. Jeong, H. C. Song, W. W. Lee, Y. Choi, and B.-H. Ryu, *J. Appl. Phys.* 108, 102805 (**2010**).
4. Z. Liu, Y. Su, and K. Varahramyan, *Thin Solid Films* 478, 275 (**2005**).
5. S. Luo, K. Wang, J. Wang, K. Jiang, Q. Li, and S. Fan, *Adv. Mater.* 24, 2294 (**2012**).
6. H. Zhang, G. Cao, Z. Wang, Y. Yang, Z. Shi, and Z. Gu, *Nano Lett.* 8, 2664 (**2008**).
7. J. Gomez and E.-E. Kalu, *J. Power Sour.* 230, 218 (**2013**).
8. A. Dziedzic and L. Golonka, *J. Mater. Sci.* 23, 3151 (**1988**).
9. X. Mei, S. J. Cho, B. Fan, and J. Ouyang, *Nanotechnology* 21, 395202 (**2010**).
10. L. P. Wang, L. Yu, R. Satish, J. Zhu, Q. Yan, M. Srinivasan, and Z. Xu, *RSC Adv.* 4, 37389 (**2014**).
11. D. Markoulides, A. Koursaris, and M. Rafferty, *Int. J. Refract. Met. Hard Mater.* 15, 123 (**1997**).
12. M. M. Hilali, K. Nakayashiki, C. Khadikar, R. C. Reedy, A. Rohatgi, A. Shaikh, S. Kim, and S. Sridharan, *J. Electrochem. Soc.* 153, A5 (**2006**).
13. H.-H. Lee, K.-S. Chou, and Z.-W. Shin, *Int. J. Adhes. Adhes.* 25, 437 (**2005**).
14. W. Songping, *J. Mater. Sci.: Mater. Electron.* 18, 447 (**2007**).
15. S. Soichi and K. Suganuma, *IEEE Trans. Compon. Packag. Manuf. Technol.* 3, 923 (**2013**).
16. S.-S. Chee and J.-H. Lee, *J. Mater. Chem. C* 2, 5372 (**2014**).
17. R. Zhang, W. Lin, K. Lawrence, and C. P. Wong, *Int. J. Adhes. Adhes.* 30, 403 (**2010**).
18. J. Y. Guo, C. X. Xu, A. M. Hu, K. D. Oakes, F. Y. Sheng, Z. L. Shi, J. Dai, and Z. L. Jin, *J. Phys. Chem. Solids* 73, 1350 (**2012**).
19. H.-S. Park, J.-Y. Hwang, E.-S. Ueon, H.-W. Kim, and M.-S. Gong, *Bull. Korean Chem. Soc.* 32, 3581 (**2011**).
20. E. B. Choi and J.-H. Lee, *Arch. Metall. Mater.* 62, 1137 (**2017**).
21. Y. Wang, Y. Zhou, W. Wang, and Z. Chen, *J. Electrochem. Soc.* 160, D119 (**2013**).
22. H. B. Lee and J.-H. Lee, *Korean J. Mater. Res.* 26, 109 (**2015**).